Value of core for reservoir and top-seal analysis for carbon capture and storage projects

Richard H. Worden

Department of Earth, Ocean and Ecological Sciences, School of Environmental Sciences, University of Liverpool, Liverpool L69 3GP, UK

0000-0002-4686-9428

Correspondence: r.worden@liverpool.ac.uk

Abstract: Carbon capture and storage (CCS) initiatives to mitigate greenhouse gas emissions are being planned in many countries, including offshore settings in the UK. To start with, almost all of these initiatives have utilized core that was originally collected to help with oil and gas exploration, appraisal and development projects. The objectives of core-based studies for CCS are subtly different to those for oil and gas studies. There are several significant reasons why core should be valued in CCS projects. Data from core provide a chance to calibrate lithology and porosity interpretations made from wireline logs that are used to characterize the subsurface and populate geocellular models. Permeability-related attributes, especially directional permeability (k_v and k_h) and relative permeability in CO_2–water mixed fluid systems, are essential to predict CO_2 injection rates and CO_2 movement patterns in the reservoir and can only be acquired from core. Although many geomechanical data, necessary to undertake safe injection of CO_2 and avoid induced fracturing, can be acquired from wireline logs, borehole imaging and downhole tests, core samples from the reservoir and top-seal are required to reveal tensile strength and to calibrate elastic and other geomechanical properties acquired from logs. Top-seal performance is critical for carbon capture and storage; core samples from top-seals are the best way to determine capillary entry pressure and so define the maximum CO_2 column height and possible CO_2 leakage rates. The possibility of dissolution reactions between formation water, acidified by high pressure CO_2, and minerals in both the reservoir and top-seal is best assessed by detailed petrographic and mineralogical study of core samples and a combination of modelling and core flow-through experiments. In summary, core is essential to CCS projects to determine CO_2 storage efficiency, CO_2 injection rates and the optimum way to safely store CO_2.

It has long been recognized that carbon capture and storage (CCS) seems to be a crucial part of the energy transition since it is going to take a substantial amount of time to wean society off fossil fuels as an energy source, and to move away from fossil fuels for use in the chemicals supply chain and as an industrial input to iron and concrete manufacture (United Nations Intergovernmental Panel on Climate Change (UNIPCC) 2005). Global warming has been closely linked to ever increasing atmospheric CO_2 concentrations, with the telling facts that the vast majority of global warming (Rohde 2021), the majority of the increase in atmospheric CO_2 concentration (Betts 2021) and even most of the change in carbon isotope ratio of atmospheric CO_2 (Graven *et al.* 2017) have all occurred since the 1960s, coincident with the vast majority of the global emissions of CO_2 (Ringrose 2020). Cutting greenhouse gas emissions is now viewed as being essential to stabilize, and then reduce, global temperatures and all the disruption to human life that increasing global temperatures would cause.

CCS is regarded as a transition technology to mitigate greenhouse gas release while we evolve to use renewable energy resources and move away from fossil fuel use in the manufacture of chemicals, iron and concrete (Lau *et al.* 2021). At the present time, the technology to supply the modern world with sufficient clean or renewable energy and material resources does not exist; thus, we will be reliant on locking up CO_2, derived from the continued use of fossil fuels, in the subsurface for many years to come. Despite the urgency of cutting greenhouse gas emissions to try to minimize the impact of induced global warming, most countries, including most of Europe, have dragged their feet in terms of establishing policy, regulation, financial incentives, government-directed research and initiatives, as well as in promoting the need for CCS and getting communities ready for the inevitable changes that will occur.

The geological part of CCS, for instance, injecting CO_2 underground for permanent disposal, has been proven by two main strands of activity. The first is the use of CO_2 for enhanced oil recovery (CO_2-EOR) (Worden and Smith 2004). Even though CO_2-EOR was originally designed to boost production rather than mitigate greenhouse gas emissions, it has been shown to leave substantial quantities of CO_2 in the subsurface, as has been reported, for example, from the Weyburn and Scurry Area Canyon Reef Operator's Committee (SACROC) oil fields (Preston *et al.* 2005; Lake *et al.* 2019). The second strand of evidence comes from the injection of

From: Neal, A., Ashton, M., Williams, L. S., Dee, S. J., Dodd, T. J. H. and Marshall, J. D. (eds) *Core Values: the Role of Core in Twenty-first Century Reservoir Characterization*. Geological Society, London, Special Publications, **527**,
https://doi.org/10.1144/SP527-2022-38

CO_2 separated from production streams from hydrocarbon fields and as a by-product of industrial processes, such as hydrogen generation and ethanol production (Global CCS Institute 2022), and injected either into saline aquifers, discrete from petroleum-bearing units, or into oil- and gas-field aquifers distant from hydrocarbon–water contacts, as has been reported, for example, from Sleipner, Snøhvit and In Salah (Ringrose 2020). Unlike EOR-related CO_2 injection, the second strand has no automatic economic benefit. A combination of financial incentives to reward or pay for subsurface disposal of CO_2 as well as financial penalties, such as Norway's CO_2 Tax Act on Petroleum Activities for release of CO_2, need to be put in place to encourage genuine CCS, as opposed to EOR-CCS, to become the norm.

Geoscience characterization for carbon capture and storage

There are many geoscience attributes that need to be defined to address specific issues linked with CCS; many of these attributes require core for either primary data or calibration of other techniques (Fig. 1). The attributes and issues that they relate to are discussed throughout this paper.

CCS involves many steps, including the collection of CO_2 from industrial and power-generation sources, CO_2 separated from petroleum streams and transportation of CO_2 via pipeline or ship to the disposal site. An injection well must be drilled and completed with appropriate metal liners to resist corrosion, especially in the lower part of the well as the liner may be in contact with high pressure CO_2 (Figs 2 & 3). The liner must be cemented in place against the penetrated rock units with cement that can withstand the presence of the acid that results from high pressure CO_2 dissolving in formation water (Mito *et al.* 2015). The completion and cementation of the injection well must be appropriate for the host reservoir to prevent formation damage at high CO_2 pressures (Carey *et al.* 2007). In the case of normally-pressured aquifers, and pressure-maintained oil and gas fields, the CO_2 is typically compressed to put it in its dense state and then it is

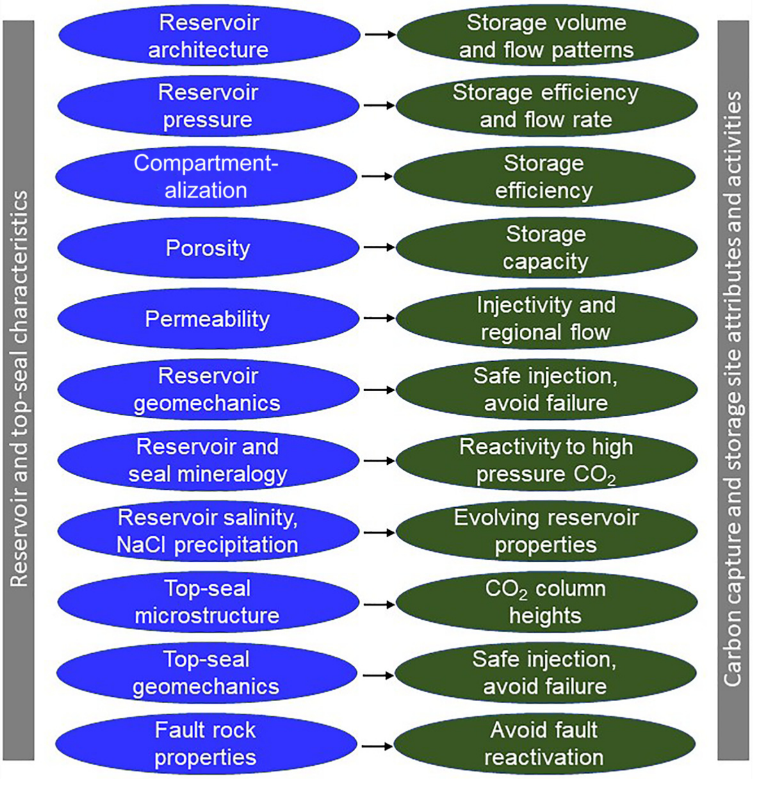

Fig. 1. Subsurface attributes for carbon capture and storage sites that need to be defined (left-hand side) and the specific questions that these attributes help to solve (right-hand side).

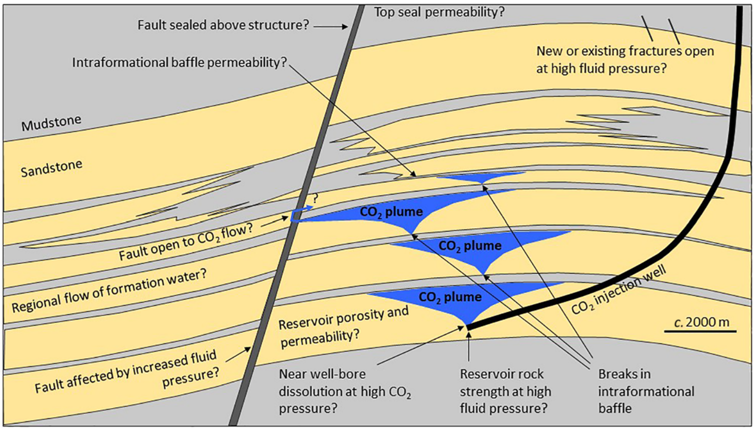

Fig. 2. Schematic geological structure used for carbon storage. Here, the CO_2 storage concept is a saline aquifer in a gentle anticlinal structure with a thick mudstone top-seal and a reservoir that contains leaky intraformational baffles. The storage domain contains variably well-connected sandstones, intra-formational mudstone barriers and possible baffles that impede but do not stop movement of CO_2. There is a risk that the major fault may be open to fluid flow; alternatively, it may inhibit movement if the fault zone contains low permeability gouge. The CO_2 issues from an injection well and, being lower density than brine, rises to the base of an intra-formational baffle. If there are breaks in the baffle, then the CO_2 will escape upwards and create a new plume. The increased fluid pressure may lead to reservoir failure in the near well-bore region. The pressure in an entire subsurface compartment will increase if CO_2 is added, possibly leading to reactivation of faults and new fractures kilometres from the injection well. The high-pressure CO_2 probably will lead to acidic formation water (pH as low as 3), and carbonate minerals in the near well-bore region may dissolve during the injection process. How much of the pore space can be filled with CO_2 (also known as the storage efficiency) depends on the initial pressure, the openness of the reservoir, the plumbing of the permeable rock units and the relative viscosity of the injected CO_2 versus the original formation water.

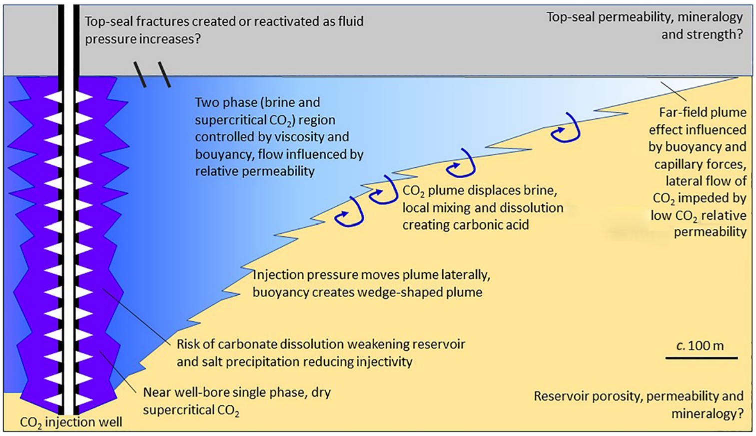

Fig. 3. Details of the fates of injected supercritical CO_2 via a single, perforated vertical well. The near well-bore region will probably be single phase, anhydrous, supercritical CO_2. The injected fluid displaces brine, controlled by differences in viscosity and relative permeability. Differences in density (buoyancy) cause the supercritical CO_2 to rise to the base of the overlying top-seal, displacing and dissolving into the formation brine. The far edge of the plume will have low CO_2 concentrations and have impeded lateral flow due to the low relative permeability scaling factor at this site. The near wellbore region risks carbonate dissolution and weakening due to low pH induced by the high-pressure CO_2. This region may also risk permeability decrease due to salt precipitation if the formation water is highly saline, as remaining brine evaporates into the dry CO_2. If pressure is not controlled to ensure that it does not exceed the fracture pressure of intact rock or, more crucially, pre-existing faults, then elevated fluid (CO_2) pressure may lead to hydrofracturing of the reservoir and creation or reactivation of fractures in the top-seal.

pumped down a borehole that terminates in a porous and permeable reservoir rock. For highly depleted gas fields, the initial stage of injection may involve injection of gas phase CO_2 to avoid Joule–Thompson cooling and the risk of high-pressure supercritical CO_2 inducing fracturing in the reservoir or top-seal (James *et al.* 2016*b*). The site must be characterized in numerous ways to ensure that the CO_2 can be injected at an appropriate rate depending on (1) the planned delivery rate from all who will supply CO_2 for subsurface disposal, (2) whether the rock is locally porous enough and regionally of sufficient volume to hold a large quantity (many megatonnes) of CO_2 and (3) whether the site is going to safely contain the injected CO_2 over a timescale of many thousands of years.

Reservoir porosity and storage efficiency

In principle, it is not a good idea to try to inject CO_2 into rocks with relatively low porosity, as the injected fluid needs to access connected pores. High porosity rocks are thus sensible target formations for CCS. However, the proportion of the pores that can be used to store CO_2 is highly variable. Storage efficiency is defined as the fraction of the available pore space that is utilized for CO_2 storage; for instance, it is the ratio between the volume of stored CO_2 and the maximum available pore volume (Okwen *et al.* 2010). Storage efficiency has been reported to be as low as 0.5% in hydrodynamically closed aquifer systems (Zhou *et al.* 2008), and as high as 70% in depleted gas fields (James *et al.* 2016*a*). Open aquifers have been shown to have storage efficiency of up to 7% (Zhou *et al.* 2008; Ringrose 2020), which is close to the predicted storage efficiency during viscous fingering during the injection of an immiscible fluid into a reservoir (Mahabadi *et al.* 2020). Storage efficiency is controlled by several factors, including the type of immiscible fluid displacement as the CO_2 plume moves in the subsurface (i.e. viscous fingering, capillary fingering or stable displacement) (Mahabadi *et al.* 2020). The relative mobility ratio of CO_2 and brine, controlled by viscosity and relative permeability, has also been used to understand storage efficiency (Nordbotten and Celia 2006). While reservoir porosity is an important variable, it is probably subordinate to pressure and architecture considerations in terms of how much CO_2 can be stored at a given site. Porosity in sandstone CCS reservoirs is typically the result of a large number of factors, including depositional and diagenetic processes (Worden *et al.* 2018). Depositional attributes include grain sorting and matrix quantity. Diagenetic processes include mechanical compaction in samples shallower than about 2500 m (i.e. a temperature less than about 60–70°C) and chemical compaction in samples from deeper than about 2500 m (i.e. temperatures greater than about 70–80°C). Mineral cements that can fill pores range from the ubiquitous carbonates, clay minerals and quartz (in deeper sandstones) to less abundant feldspars, anhydrite and pyrite. Porosity can be approximately predicted based on knowledge of depositional environments, primary texture, bioturbation (and other early diagenetic processes) and the burial and thermal history.

Reservoir pressure and storage efficiency

Reservoir pressure plays a major role in CCS projects. The injected CO_2 ideally must not exceed the fracture pressure of the reservoir, or top-seal, as damaging these two rock types may respectively inhibit injection and compromise the integrity of the storage volume (Ringrose 2020). Injectivity is partly a function of the difference between reservoir pressure and bottom hole pressure.

If the reservoir is normally pressured (either a saline aquifer or a pressure-supported depleted oil field), and close to the fracture pressure, then the ability to increase the bottom hole pressure will be limited, assuming that hydro-fracturing must be avoided. Conversely, if the reservoir is a depleted gas field, then the reservoir pressure before CCS starts may be lower than hydrostatic pressure. Low reservoir pressure may help both injectivity and storage efficiency (Hughes 2008), although initial injection of CO_2 may need to be in the (low density) gas phase to prevent Joule–Thompson cooling (Oldenburg 2007). In depleted gas fields, it may also be necessary to take care to avoid exceeding the post-depletion reservoir fracture pressure, which may be lower than the virgin reservoir fracture pressure (Santarelli *et al.* 1999; Kaldi *et al.* 2011).

Reservoir permeability and injectivity

The permeability of a CCS reservoir has a direct impact on the rate at which CO_2 can be injected, also known as injectivity. For an idealized (vertical) cylindrical reservoir with minimal heterogeneity, injectivity is proportional to permeability (Miri and Hellevang 2019). Given a range of CO_2 reservoir options, it might be advantageous to select a reservoir with the highest permeability to facilitate easiest injection. However, given that fluid flow properties of rocks have directionality, it may be important to consider vertical and horizontal permeability and stratigraphic variations of permeability, as these will influence how and where the CO_2 moves in the subsurface. Permeability is controlled by primary sediment attributes and many post-depositional processes, including all the factors that control porosity but also depositional grain size and the form of mineral cements that reduce porosity. For example, pore-filling cements tend to have a bigger impact on permeability than grain-coating cements (Cade *et al.* 1994). Permeability can be approximately predicted based on knowledge of porosity, style of cement growth, textural attributes of the rock and burial and thermal history.

The ability of a fluid to flow through a porous matrix in the presence of a second, immiscible fluid is known as relative permeability (Cannon 2016). Relative permeability is a scaling factor, between one and zero, by which the absolute permeability is multiplied to give the effective permeability. The volumetrically-dominant fluid usually has the highest relative permeability scaling factor, but the relationship between movement of mixed fluids through pores also depends on the wetting preference of the mineral matrix for one fluid or the other. Paired with saline brine in a sandstone matrix, CO_2 is typically the non-wetting phase resulting in the granular matrix retaining residual (irreducible) CO_2 once plumes have moved by, thus limiting the ability of CO_2 to flow, especially at low CO_2 (high water) saturations (Krevor *et al.* 2012; Burnside and Naylor 2014).

Structure of the subsurface storage site

Injected CO_2 is trapped in four main ways: in a structural or stratigraphic trap as the dominant fluid phase (Figs 2 & 3), as residual immiscible fluid droplets in predominantly brine-filled pores once the main CO_2 plume has passed, by dissolving in formation water (brine) and by precipitating as carbonate minerals, typically after thousands of years (UNIPCC 2005). The physical structure of the subsurface, geological faults, folds and details of heterogeneous stratigraphy strongly influence where and how CO_2 is structurally or stratigraphically trapped.

Reservoir architecture and intraformational baffles

All reservoirs have some degree of heterogeneity in terms of permeability; most reservoirs contain intraformational baffles, such as clay-rich intervals or even thin, interbedded mudstones. These baffles may result in separation of the storage site into discrete pockets, which may result in discrete CO_2 accumulations (Fig. 2) such as those found in the Sleipner CCS site (Cavanagh and Haszeldine 2014; Williams and Chadwick 2021). Depositional connectivity of good quality sandstone may also influence compartmentalization. High resolution seismic images were used to explain CO_2 movement patterns at the Snohvit CCS site (Hansen *et al.* 2013). Depositional channel structures also have strongly influenced CO_2 movement patterns in the various sand bodies that comprise the Utsira Formation at the Sleipner CCS site (Williams and Chadwick 2021). The presence of baffles and poor reservoir quality sandstone, their geographical distributions and local gaps in baffles are therefore important attributes of a CCS site.

Reservoir geomechanical properties and stability of existing faults

How the reservoir physically responds to the injection of CO_2 at high pressure depends on elastic and inelastic geomechanical attributes. If the CO_2 fluid pressure exceeds the fracture pressure of the reservoir in the near-wellbore region, then the reservoir will fracture. Induced fracturing is an advantage for production from low permeability unconventional reservoirs but is not considered to be desirable at CCS sites due to the risk of damaging the top-seal. Fracturing, induced by high fluid pressure, was identified as the cause of increased injectivity at In Salah, showing that exceeding fracture pressure in the reservoir is not detrimental to every aspect of a CCS project (Goertz-Allmann *et al.* 2014). It has been shown that CCS causes reservoir fluid pressure to increase far away from the CO_2 plume (Rutqvist *et al.* 2010), potentially leading to reactivation of existing faults and possibly creation of new fractures. Evidence for CCS-induced fractures comes from microseismic monitoring, which has revealed the occurrence and frequency of fracturing events (Verdon *et al.* 2011). Some CCS projects seem to be associated with a distinct increase in the frequency of seismic activity (Lescanne *et al.* 2011; Goertz-Allmann *et al.* 2014; Worth *et al.* 2014; Verdon 2016), demonstrating that a minor degree of earthquake activity may, in some cases, be an inevitable consequence of CCS. It was reported that injection of water and CO_2 for enhanced oil recovery both caused microseismic events, so that it is not so much the type of fluid as the pressure increase that is important (Verdon *et al.* 2010).

Reservoir mineral response to CO_2 injection

CO_2 at high partial pressure (mole fraction of CO_2 times overall fluid pressure) leads to low pH (acidic) brine (Plennevaux *et al.* 2013). Some minerals, such as carbonate minerals (calcite, dolomite and siderite), and chlorite (an Fe–Mg-rich clay mineral) can rapidly dissolve in mildly acidic brine (Armitage *et al.* 2013*a*). Reports of produced formation water (brine) chemistry from CO_2-enhanced oil recovery (CO_2-EOR) projects have shown that calcium and other metals associated with carbonate cements tend to increase over the course of a few months of CO_2-EOR, leading to the conclusion that dissolution of some components in the reservoir occurs on an engineering timescale (Worden and Smith 2004; Mito *et al.* 2008; Shevalier *et al.* 2013). The artificially induced acidity resulting from CCS will thus lead to localized dissolution of calcite, dolomite, siderite and chlorite, if they are present in the reservoir. Dissolution may be most concentrated in the near-wellbore region, possibly leading to a localized increase in porosity and consequent change in geomechanical properties, probably weakening, of the reservoir. Mineralogy and rock fabric may be aspects that need to be factored into the assessment of the effects of CCS on the host reservoir.

In contrast to the effects of mineral dissolution, CO_2 injection into reservoirs that contain highly saline brines has been shown to lead to halite precipitation and a consequent decrease in injectivity (Grude *et al.* 2014; Miri *et al.* 2015). Injected CO_2 is typically anhydrous so that when the dry CO_2 meets saline formation brines, some of the H_2O in the brine evaporates into the brine leading to ever increasing salinity of the remaining brine; once halite saturation is reached, halite starts to precipitate in pores and pore throats (Miri and Hellevang 2016). Halite growth is partly facilitated by capillary backflow of dissolved NaCl, via irreducible water, which occurs preferentially in finer-grained, lower-permeability rock (Miri *et al.* 2015). Facies identified from core is thus valuable in helping identify where halite precipitation may occur.

Top-seal and fault-seal petrophysical properties

Oil and gas fields always have a low permeability top-seal that has trapped the petroleum fluids for millions of years. Top-seal properties have been relatively little studied compared to reservoir properties simply because the top-seal can be assumed to be effective if a petroleum column is present, although the penetrations by exploration, appraisal, production and injection wells provide a minimum of wireline log and cuttings data to assist with top-seal characterization (Jahn *et al.* 2008). If a saline aquifer is to be used for a CCS site, the same assumption cannot necessarily be made for whatever lithology is sitting on top of the CO_2 reservoir rock. The ability of the top-seal to contain high pressure CO_2 is a consequence of the pore fabric of the rock, that in turn controls average pore throat radius, capillary entry pressure and permeability. Top-seal properties tend to improve in older and more deeply buried formations (Espinoza and Santamarina 2017) that have undergone more compaction and diagenetic mineral transformations. Top-seal geomechanical properties also need to be considered; if the top-seal is likely to fracture as fluid pressure increases, then this may compromise the seal's integrity. Depleted oil and gas fields planned for CCS present a different type of geomechanical challenge, as the cycle of depressurizing during petroleum production followed by re-pressuring during CCS may lead to unexpected consequences, such as reduction in minimum horizontal stress and thus fracture pressure (Shin and Santamarina 2017), and development of new CO_2 leakage pathways through top-seals along wellbores if the reservoir collapsed during depressurization (Santarelli *et al.* 1999; Kaldi *et al.* 2011).

Faults usually form arrays that can displace both reservoirs and top-seals. Faults, including those in CCS systems, may result from several processes, such as far-field plate motions, folding, gravitational sliding and crustal unloading associated with uplift. Faults and fractures may enhance or retard the rates of fluid migration. The impact of faults and fractures on CO_2 migration is affected by three issues. The first issue includes the orientation of faults and fractures in the reservoir and caprock relative to the stress field (Zoback 2007). The second issue is whether faults and fractures affect (positively or negatively) the movement of CO_2 during and after injection. The third factor is whether natural or injection-induced stresses influence the behaviour of these faults and fractures. To address these issues, it is necessary to understand the main properties that control whether a fault will act as a conduit for CO_2 movement or behave as a seal. These diametrically opposed behaviours depend on juxtaposition of beds (the physical displacement of sealing rocks against reservoir rocks), fault zone effects (grain sliding, cataclasis, cementation, shale gouge/clay smear) and reactivation of faults (due to changes in fluid pressure leading to fault movement and the creation of structural permeability and new fluid migration pathways) (Kaldi *et al.* 2013).

Top-seal mineralogical response to CO_2

The acidity that results from CCS may lead to reaction with minerals in the top-seal, especially in saline aquifers where the storage efficiency is relatively low and the dominant but newly acidic residual water in the reservoir can be in contact with the top-seal. As with reservoirs, carbonate minerals and chlorite in top-seal mudstones are susceptible to dissolution so the mineralogy of the top-seal may be an important consideration (Worden *et al.* 2020*a*). For example, if a top-seal mudstone is calcite-bearing, then it may undergo calcite dissolution when in contact with high pressure CO_2 (Wolf *et al.* 2016). In contrast, if a top-seal mudstone is quartz- or illite-bearing, then it will be largely unaffected by the acidity induced by CO_2 injection (Worden *et al.* 2020*a*).

Dissolution of minerals in top-seals due to reaction with CO_2 has been shown to occur in a matter of days using experiments and geochemical reaction path modelling (Szabo *et al.* 2016); dissolution of carbonate minerals was observed and feldspar dissolution was inferred from models, with both leading to secondary carbonate and clay mineral formation. The consequence of CO_2 injection was primarily the increase of mineral dissolution rates, but the effect on the pore network seems to be uncertain (Szabo *et al.* 2016).

Conversely, smectite-bearing top-seal mudstones may undergo net solid volume increase when subject to high pressure CO_2 since the interlayer sites in smectite can adsorb CO_2 (Loring *et al.* 2019), leading to 'smectite swelling stresses' (Zhang and Wu 2019). Clay swelling in a fractured top-seal mudstone may cause fault reactivation and leakage of CO_2 from the reservoir if the faults have offsets similar to the top-seal thickness, if creep cannot mitigate swelling stresses and if the fault is sufficiently permeable (Busch *et al.* 2020).

Role of core in the geoscience characterization for carbon capture and storage

Several of the geoscience issues described previously can be best addressed by core-based studies. Seismic data, wireline log data, drilling rate data, well test data – including bleed-off, leak-off, formation testing by downhole tools and downhole pressure measurements – are all essential to develop a holistic understanding of the CO_2 reservoir and containment system (top-seal and fault-seal), but the value of core also needs to be appreciated.

Lithology analysis and cores

The focus on reservoir sedimentology and sequence stratigraphy that has developed over the last 40 or 50 years of oil field exploration and appraisal may not be wholly maintained for the growing CCS industry, unless there are vital reservoir architecture-related questions to be addressed by examining intact rock samples that cannot be answered by seismic data, wireline log data, drilling rate data, well test data and downhole pressure measurements. Despite this, the vast number of legacy wells that have core will serve as an enormously valuable resource for better understanding the lithology of future CCS reservoirs. It is important that all existing core, for any possible future CCS reservoirs, is correctly preserved for the benefit of future projects as we pursue the energy transition.

Lithology can be interpreted by analysis of routine wireline logs such as the gamma, density, sonic, neutron and resistivity logs, assisted by less common tools such as nuclear magnetic resonance (NMR) and geochemical logs (Rider and Kennedy 2011) (Fig. 4). Bedding can be visualized using micro-resistivity and other imaging tools. This approach can reveal the presence of reservoir, top-seal, intraformational baffles, cemented nodules or horizons and reservoir zones with reduced reservoir quality due to non-radioactive clay minerals such as kaolinite or chlorite. However, core is essential for ground-truthing the log-derived lithology analysis by providing the opportunity for calibration.

When selecting reservoirs for CCS projects, reservoirs will typically be chosen that are deep enough to place the CO_2 in the super-critical phase, i.e. >850 to 1000 m (Doughty *et al.* 2008; Ringrose 2020) but shallow enough (1) to avoid expensive deep wells that would require high cost compressors, and (2) for the sandstones to have good reservoir quality. Under some circumstances, reservoirs that are sedimentologically simple may also be preferentially selected for CCS (e.g. Fig. 5a, b), making core description less important than it would be for complex (i.e. strongly heterogeneous) reservoirs. However, greater sedimentological complexity, making reservoir and core description more important, may lead to higher storage efficiency. On balance, detailed sedimentological description and interpretation based on cores probably remains as important for CCS as it is for petroleum exploitation.

Reservoir porosity, permeability, flow simulation models and cores

Reservoir porosity data, needed for the calculation of CO_2 storage capacity (Fig. 1), can be acquired from careful use of wireline logs such as the density, sonic and neutron logs (Rider and Kennedy 2011) (Fig. 4). However, porosity data acquired from core permit essential calibration and ground-truthing of the wireline log porosity data (Fig. 4). The close agreement between the log and the core porosity data shown in Figure 4 reveals that the log data can be highly credible; the log data have been able to pick out the two low porosity zones in the reservoir. The upper zone is associated with a gamma spike and, in the absence of core, could be interpreted to be an intraformational shale. The lower zone has no gamma spike and so cannot be a shale; this zone has a low sonic log signal and may be interpreted to be a carbonate (probably calcite) cemented layer or nodule (Kelly *et al.* 2022). The interpretation of the lower porosity zone being due to calcite can only be confirmed by core description, which would thus reduce interpretation uncertainty. Whether the calcite is a layer or nodule has important ramifications for compartmentalization of the reservoir; although wireline logs do not provide information about this issue, examination of core may reveal a curved outline of the calcite cemented zone, typical

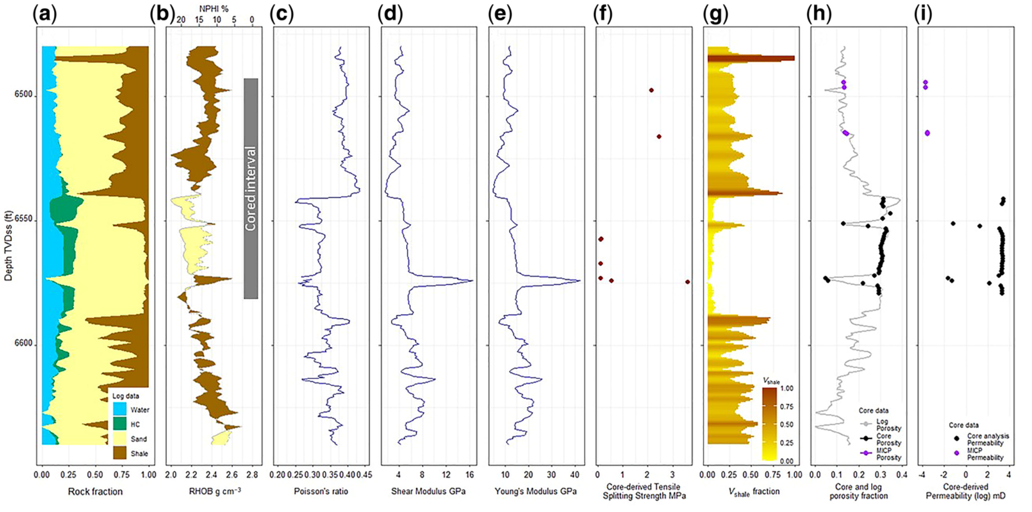

Fig. 4. Log and core data from well 14/26a–7A through the Lower Cretaceous Captain Sandstone and the overlying Rodby Shale, Moray Firth Basin, UK, with the data harvested from the Oil and Gas Authority's National Data Repository. (**a**) Simple lithology log derived from the density log (porosity) and the gamma log, which was used to split the solid fraction between sand and shale. Porosity was split into oil and water-bearing proportions using the resistivity log and a modified version of the Archie equation. (**b**) Neutron density cross-over diagram revealing net reservoir (yellow) and non-reservoir (brown). Cored interval indicated. (**c**–**e**) Elastic geomechanical properties derived from compressional and shear sonic logs and the density log (Rider and Kennedy 2011). (**f**) Inelastic properties (tensile splitting strength) derived from geomechanical tests on core (Allen *et al.* 2020). (**g**) V_{shale} log derived from the gamma log, assuming that shales are dominated by radioactive K-bearing illite. (**h**) Core analysis-derived porosity (reservoir) and mercury intrusion-derived porosity (top-seal) compared to density-log-derived porosity. (**i**) Core analysis-derived permeability and mercury intrusion-derived permeability from top-sealing mudstones. The combination of log- and core-derived data provide a detailed picture of the reservoir and top-seal required to store CO_2.

of a non-compartmentalizing nodule. Petrographic and geochemical studies of core-derived samples may further help resolve the calcite nodule or calcite layer interpretation (Kelly *et al.* 2022). In summary, although good quality porosity logs can be used to describe porosity distribution, core data are essential to define what controls porosity and to calibrate log porosity.

Permeability data, needed for the calculation of CO_2 injectivity (Fig. 1), are not typically available directly from wireline log data unless NMR logs have been run, although note that NMR logs should be calibrated to relevant core samples. Core is typically essential to gain a quantitative appreciation of both average reservoir permeability, the way permeability varies throughout the reservoir, and permeability-anisotropy (Fig. 4). If there is a well-understood relationship between porosity and permeability for a given suit of rocks, then it may be possible to derive permeability from porosity-derived wireline logs. However, core is typically needed to develop the reservoir-specific understanding of the relationship between porosity and permeability (Worden *et al.* 2018). The Captain Sandstone in the Moray Firth is a high-quality reservoir, with porosity values typically greater than 25%. However, average core analysis permeability decreases systematically with depth (Fig. 6) from about 2000 mD in the shallowest reservoirs to the NW of the play to about 1000 mD in the deepest reservoirs to the SE. This variation of average permeability represents a halving of the CO_2 injection rate, with all other factors remaining the same (Fig. 7). Note also that each depth interval has a substantial range of permeability values, reflecting dynamic reservoir permeability; these ranges represent zones that would have substantially different CO_2 flow rates within the injection zone. In summary, core is essential to characterize reservoir permeability unless NMR logs are available, although NMR logs need to be calibrated and ground-truthed to core analysis data. Legacy core may be sufficient in the case of well characterized systems, but new core may be needed if adequate reservoir (permeability) characterization is to be achieved.

Not only is it important to know the overall reservoir permeability, but it is also important to know how it varies stratigraphically (Fig. 4), and what controls permeability in order to develop a method to predict permeability and populate geocellular models. Figure 8 illustrates an example of good quality

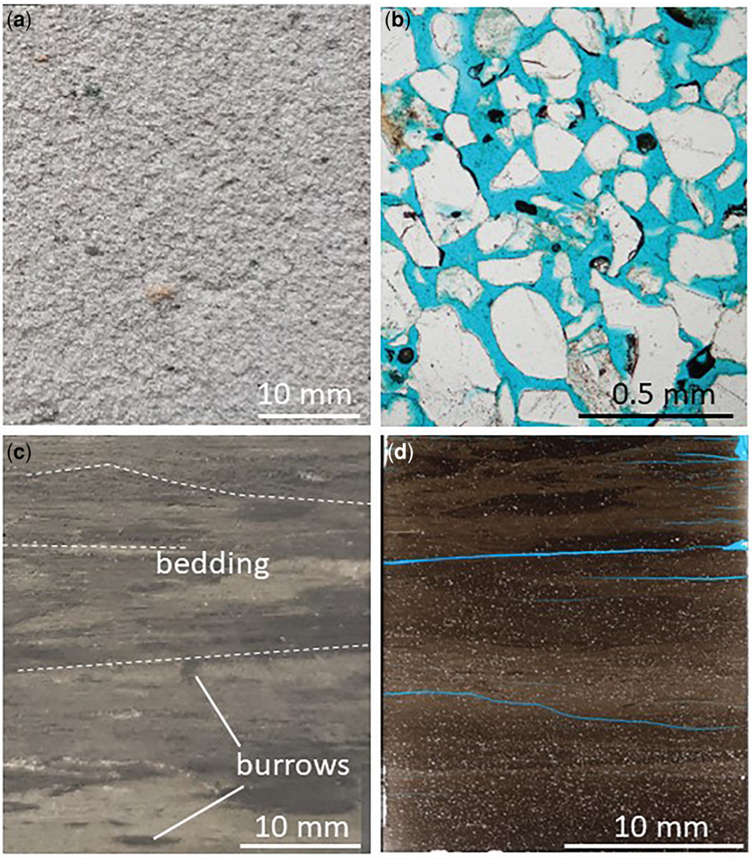

Fig. 5. Core images of Captain Sandstone and Rodby Shale, which are the CCS reservoir and top-seal to the planned Acorn site. (**a**) Image of slabbed core from reservoir revealing the typical appearance of the core: it is a relatively bland and structureless sandstone (Allen *et al.* 2020). (**b**) Thin section image of the highly porous Captain Sandstone. The pores are blue, as the sample was injected with blue-dyed resin. (**c**) Image of slabbed core of the Rodby Shale revealing a high degree of heterogeneity, including primary bedding (white dashed lines as examples) and secondary bioturbation fabrics (burrows indicated). (**d**) Thin section image of Paleocene Lista Shale top-seal revealing bedding picked out by light and dark layers. The heterogeneous speckling is caused by variable quantities of silt, in this case dominated by quartz (Worden *et al.* 2020*a*). The blue cracks in the thin section are resin-filled artefacts resulting from sampling and preparation.

reservoir from the Paleocene Mey Sandstone Member, part of the Lista Group, that displays a weak correlation of permeability with porosity. Instead, permeability is controlled by grain size, and to a lesser extent, by sorting. Studies show that permeability in different reservoirs can be controlled by a range of factors, such as matrix content, pore-filling cements and secondary porosity. In this example (Fig. 8), only core-derived measurements could reveal that the primary controlling factor is grain size. It is possible to conclude that core is essential to understand permeability, and thus injectivity, at CCS sites.

The relative permeability scaling factor is different for each combination of fluid and rock type. The main fluid variables are the ratio of brine to CO_2, and the composition of the brine. The main rock variables are mineralogy, specifically the minerals facing the open pore, and rock fabric. Relative permeability must be determined using core samples, as illustrated in Figure 9. Core is thus essential for the calculation of CO_2 movement patterns in CCS sites.

Simulation of the effects of both short-term injection (Williams and Chadwick 2021) and long-term CO_2 flux distant from the injector well (Dean and Tucker 2017) has been employed to reveal how CO_2 will behave in the subsurface, and the effects that the CO_2 has on factors such as geomechanical (Williams *et al.* 2016) and mineralogical (Wolf *et al.* 2016) properties of the reservoir.

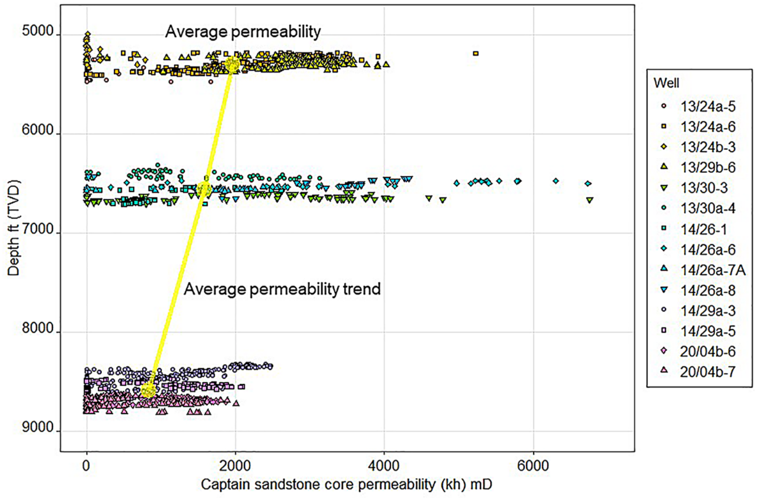

Fig. 6. Core analysis permeability v. depth for the Lower Cretaceous Captain Sandstone with average permeability calculated for the three depth intervals. There is a typical range of permeabilities at each depth due to variable quantities of clay and carbonate cement. The average permeability decreases with depth are due to compactional porosity loss. Source: data taken from the National Data Repository.

Dynamic models required to simulate fluid (i.e. CO_2 and the pre-injection fluids) movement need to have grid blocks populated with dynamic properties that influence fluid flow, such as permeability (both horizontal and vertical) and relative permeability. The spatial and stratigraphic distribution

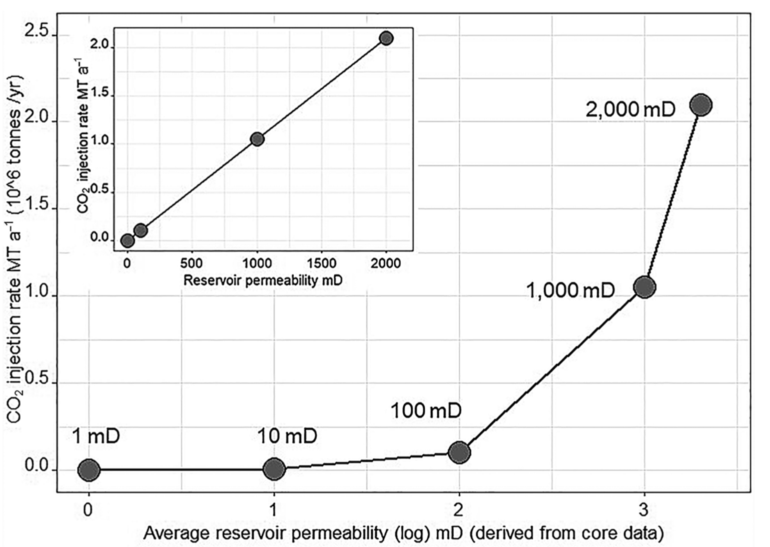

Fig. 7. Modelled variation of injectivity as a function of average reservoir permeability, using the approach of Miri and Hellevang (2019). Main graph shows log permeability with the inset plotting the same data on a linear scale to illustrate the simple relationship between mean permeability and injection rate. The model assumptions include: reservoir fluid pressure of 27 MPa (3916 psi), the bottom hole CO_2 injection pressure of 30 MPa (4351 psi), the reservoir is 100 ft (30.5 m) thick and homogeneous, the injection well has a 6 inch (15.25 cm) radius, the reservoir has a radius of 2000 ft (609 m), CO_2 viscosity is 0.085 cp (equivalent to 0.085 MPa.s) and CO_2 density is 600 kg m^{-3} (6.013 pounds/imp. gall). Permeability data derive primarily from averaging core analysis data, although NMR-log-derived permeability data could also be used if NMR tools were employed. The plot reveals that injectivity progressively increases with reservoir permeability, which is normally taken from core analysis data.

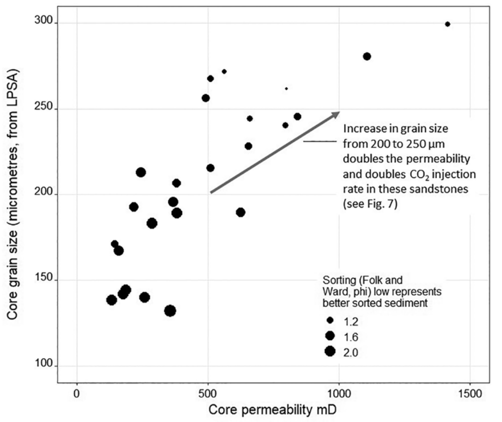

Fig. 8. Illustration of how core-derived data can help to reveal the fine controls on permeability for the Paleocene Mey Sandstone Member of the Lista Group, Moray Firth, UKCS, planned for CCS. Permeability data were derived using conventional core analysis methods from core; grain size and sorting were derived from the same depth interval as the core plug, using laser particle size analysis (LPSA). Grain size has a dominant control on permeability with sorting playing a subordinate role. There is no correlation between porosity and permeability for these good quality sands. These core-derived data show that the CO_2 injection rate into 250 µm grain size sandstone will be about twice that of injection into 200 µm grain size sandstone.

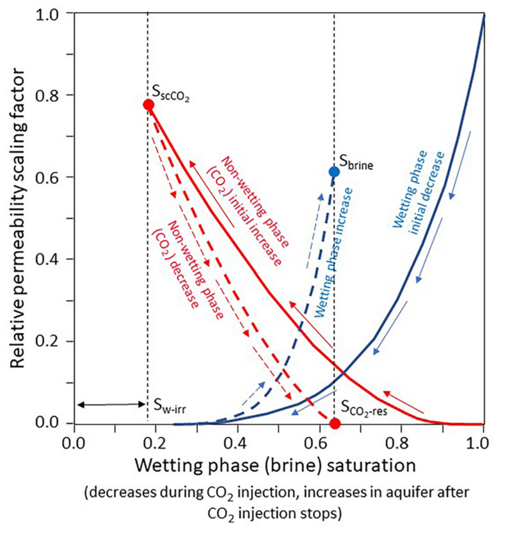

Fig. 9. Typical CO_2 and brine, core-derived, relative permeability curves representing initial CO_2 influx (wetting phase brine decrease) followed by water influx (wetting phase increase) here for a typical sandstone (Burnside and Naylor 2014). The lab-measured absolute permeability from core must be multiplied by the relative permeability scaling factor to get the effective permeability of the rock to each fluid. As CO_2 concentration decreases, its rate of flow will decrease, with all other factors remaining constant. This diagram shows that at the far-field part of the plume, where CO_2 concentration is low, the CO_2 will not be able to flow as the relative permeability scaling factor drops to zero. The residual S_{scCO_2} is the maximum initial saturation of supercritical CO_2 after a decrease of the wetting phase brine. S_{CO_2irr} is the residual CO_2 saturation after brine comes back into the rock. S_{wirr} is the irreducible brine saturation after flooding with supercritical CO_2. S_{brine} is brine saturation after brine comes back into the rock. The diagram also explains the concept of residual CO_2 trapping; the relative permeability scaling factor of CO_2 is zero (CO_2 cannot flow) at S_{CO_2irr} even when there is approximately 36% CO_2 in the pore system. Relative permeability curves and the value of S_{CO_2irr} therefore explain why residual CO_2 trapping occurs.

of directional permeability and relative permeability (and porosity and other variables) of the reservoir and the sealing units are typically input into a geologically-realistic representation of the reservoir, known as a static model. In terms of workflow, static models are developed first, and then used as input for the dynamic modelling software. Static models are typically developed utilizing sedimentological, structural, petrophysical and geomechanical data as well as concepts derived from seismic, wireline and core data. Core-logs (grain size, primary sedimentary structures, bioturbation type and extent as well as diagenetic fabrics) are essential to ground-truth the sedimentological concept used to help populate the static model with different facies types (Williams and Chadwick 2021). Core analysis data, especially permeability and relative permeability, are essential to build the understanding of how different facies types will allow CO_2 and other fluids to move once injection commences (Marshall *et al.* 2016). Core-derived geomechanical data are important in poro-elastic simulation models for developing an understanding of how different facies will physically respond to changing fluid pressure (Rutqvist *et al.* 2010). Core samples are also needed to produce mineralogy and grain size (i.e. specific surface area) data for each mineral if flow and geochemical reaction models are going to be created (Xu *et al.* 2007; Wolf *et al.* 2016).

Reservoir strength and cores

In order to address geomechanical stability, it is necessary to establish the magnitude and orientations of the three principal stresses and understand the elastic properties of the reservoir and top-seal. The magnitude and orientation of maximum, intermediate and minimum principal stresses can be determined or estimated by a combination of density log data converted into vertical effective stress, leak-off tests for minimum horizontal stress and wellbore breakout, borehole imaging and mini-frac tests for the orientation of maximum and minimum horizontal stresses (Gaarenstroom *et al.* 1993; Zoback 2007; Gholami *et al.* 2021).

Elastic properties of rocks, such as Poisson's ratio and Young's modulus, can be determined using high-quality wireline log suites that include a density log and compressional and shear sonic logs (Rider and Kennedy 2011). There are also established relationships that allow rock properties, such as tensile strength and unconfined compressive strength, to be predicted from elastic properties derived from combined wireline logs (Chang *et al.* 2006) or directly from sonic logs (Liu 2017). Core and lab-based methods are needed to calibrate log-derived elastic and inelastic properties. Although wireline logs can theoretically be used to determine the conditions under which reservoir rocks at CCS sites might fail, the relationships are not wholly understood. It is known that porosity (Chang *et al.* 2006) and mineralogy (Rybacki *et al.* 2015, 2016) influence rock strength, but links of rock strength to specific variables such as grain size, sorting, grain shape and degree and type of diagenetic alteration are not yet understood. Figure 10 is a schematic illustration of the effect of calcite cement on Young's modulus (and porosity and permeability). The geomechanical understanding of CCS sites is of paramount importance to ensure that injection rates are as high as possible to achieve good efficiency, but not too high to cause failure (hydro-fracturing) of the reservoir. On this basis, it is likely that core samples will be required (Fig. 4) to allow direct measurements of rock strength from key horizons (reservoir and top-seal), to ensure that fracture pressure is not exceeded during CO_2 injection. Core-based studies should go beyond simple measurements of rock strength from core by including measurements of grain size, sorting, grain shape and degree and type of diagenetic alteration (Blake *et al.* 2022). Comparison of geomechanical with sedimentary and diagenetic data promises to lead to high credibility predictions of rock strength at CCS sites.

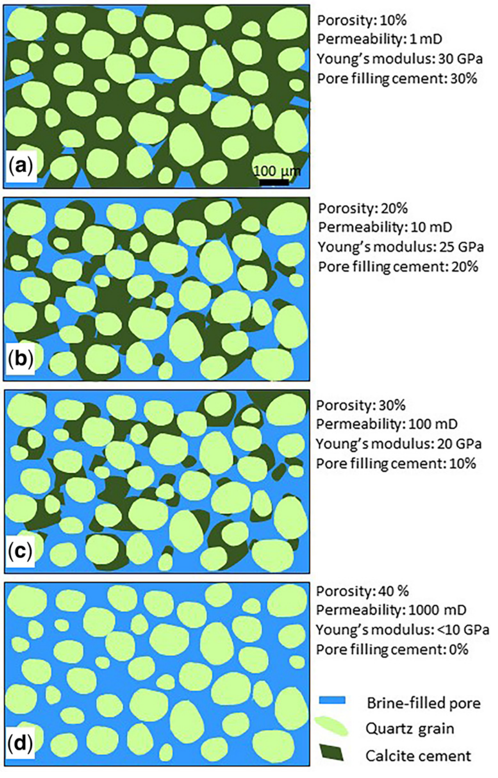

Fig. 10. Schematic illustration (based on data from Fig. 4) as to how cement quantity has a direct effect on geomechanical properties such as Young's modulus, and petrophysical properties such as porosity and permeability. The sequence (**a**) to (**d**) represents progressively less cement, higher permeability and porosity and lower Young's modulus.

Reservoir reactivity and cores

Field- and lab-based studies have shown that injecting CO_2 into porous rocks can lead to mineral dissolution, specifically in calcite-cemented sandstones and carbonate reservoirs, but probably less likely in quartz-cemented sandstones (Vilarrasa *et al.* 2019). Field-based studies have shown that the dissolved concentration of elements such as Ca typically increases during CO_2-EOR projects (Worden and Smith 2004; Mito *et al.* 2008; Shevalier *et al.* 2013). Lab-based studies simulating influx of CO_2, many using core, have shown that calcite dissolves (Hangx *et al.* 2013; Yang *et al.* 2017; Singh *et al.* 2018) and porosity and permeability thus increase (Vanorio *et al.* 2011; Nover *et al.* 2013; Dawson *et al.* 2015; Singh *et al.* 2018; Wei *et al.* 2020) (Fig. 11).

Increasing the porosity, and thus permeability, of the reservoir in the near-wellbore area has important ramifications for injectivity; the ability to inject CO_2 into the reservoir may improve. However, if the rock dissolves too much, it may substantially alter the geomechanical properties of the reservoir. It can be expected that CO_2-reactive reservoir rock will become weaker and may undergo fracturing or collapse during shut-in periods, thus, potentially limiting injectivity and so requiring an appropriate well completion that circumvents this problem. Despite advances in log analysis, it can be difficult to determine the presence of small quantities of calcite in sandstone, although the presence of wholly calcite-

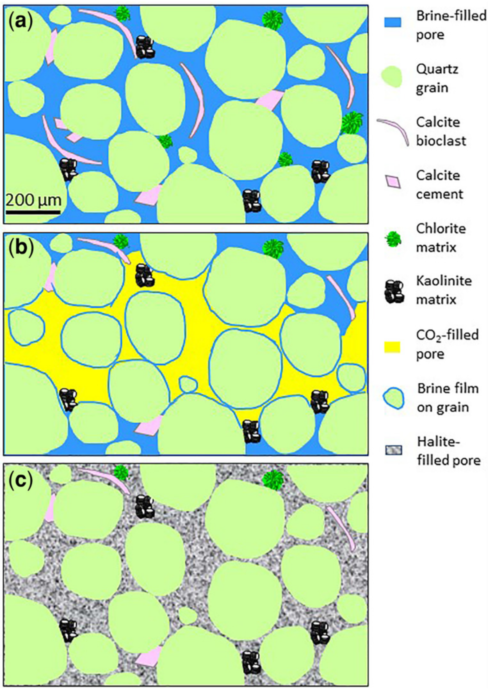

Fig. 11. Representations of a typical sandstone before CO_2 injection, during CO_2 injection and following halite precipitation induced by evaporation of H_2O from the pre-existing saline brine into the CO_2 (**a**) Schematic representation of moderately compacted quartz-rich marine sandstone with calcite bioclasts, calcite cement, chlorite-rich matrix and kalinite-rich matrix. The pore space was initially filled with brine. (**b**) Schematic representation of the effect of flowing supercritical CO_2 with only some of the pores occupied by CO_2 (based approximately on Iglauer *et al.* 2019), the remainder being filled with brine. Quartz grains in the CO_2 plume are water-wet leaving them with a film of brine between the CO_2 and the grain. Calcite bioclasts and cement and the chlorite-matrix have dissolved where in contact with the acidic CO_2–water mixture (based on Armitage *et al.* 2013*a*), changing the metal chemistry of the brine (Worden and Smith 2004) and leading to increased porosity (Alam *et al.* 2011). The calcite and chlorite in the water-filled pores may eventually dissolve due to diffusive flux of CO_2 into the water, leading to decreasing pH. (**c**) Schematic representation of the sample shown in Figure 5b after precipitation of microcrystalline halite in situations where the original formation water (brine) is relatively saline (Miri and Hellevang 2016). The halite leads to a decrease in CO_2 injectivity as the pore throats in the near well-bore region become plugged; note that this reservoir scaling problem can be remedied by episodic injection of methyl ethyl glycol (Grude *et al.* 2014).

cemented layers or nodules can usually be detected (Fig. 4). Cuttings can be used to determine mineralogy of a reservoir, although use of cuttings has limited vertical resolution and cuttings tend to be mainly composed of the most indurated (cemented) types of rock in the reservoir, and therefore might not be representative of the reservoir as a whole. It is thus essential to have core from clastic CCS reservoirs to map out the type and distribution of calcite cement, and other potentially reactive minerals. Examples of variably calcite-bearing rocks are presented in Figure 12, with the importance of mineralogy and rock texture on reservoir and top-seal porosity illustrated in Figure 13. Finely detailed petrographic descriptions of intact samples and quantitative petrographic data cannot be acquired from cuttings and wireline logs. Core is therefore needed to undertake studies of the occurrence of reactive minerals in reservoirs, and to determine where in the reservoir such minerals occur. Minerals other than carbonates may also react with CO_2 in the presence of brine; for example, experimental work showed that chlorite (Mg–Fe silicate clay; Fig. 11) and siderite (Fe–carbonate) both underwent extensive dissolution as a result of CO_2 injection (Armitage *et al.* 2013*a*; Worden *et al.* 2020*b*).

Carbonate mineral precipitation is rather less likely to occur than mineral dissolution on CCS engineering timescales, although mineral trapping is viewed as the safest long-term fate of CO_2 (UNIPCC 2005). However, modelling injection of CO_2 at the Heletz CCS site in Israel revealed growth of *c.* 2% anhydrite as a result of *c.* 3% dolomite dissolution. The released Ca from dolomite dissolution tipped the formation brine into a supersaturated state with respect to anhydrite; overall, there was a modelled minor net increase in porosity in the reservoir at Heletz (Wolf *et al.* 2016). Chlorite, a common Mg- and Fe-rich clay mineral in some sandstones, is a source of divalent metals that may react with CO_2 to create new Mg and Fe carbonate minerals (Sundal and Hellevang 2019; Worden *et al.* 2020*b*). Note that injection of CO_2 into fractured vesicular basalts at the CarbFix projects in Iceland has proved successful at creating new carbonate minerals instead of free CO_2 within a few years, because basalts contain an abundance of minerals (e.g. anorthite, clinoproxene, orthopyroxene and olivine) with divalent cations (e.g. Ca, Mg and Fe) that are capable of creating carbonate minerals (Snaebjornsdottir *et al.* 2017, 2018; Clark *et al.* 2020). Sandstones and carbonates seldom contain an abundance of reactive minerals, so the basalt-CCS case cannot be used as a model for CO_2 injection into sedimentary rocks. Core samples are important for the identification of minerals that may dissolve and lead to growth of new secondary minerals, such as anhydrite, and to map out the type and distribution of chlorite in sandstone reservoirs in order to predict the potential for sandstone to lock up CO_2 by mineralization.

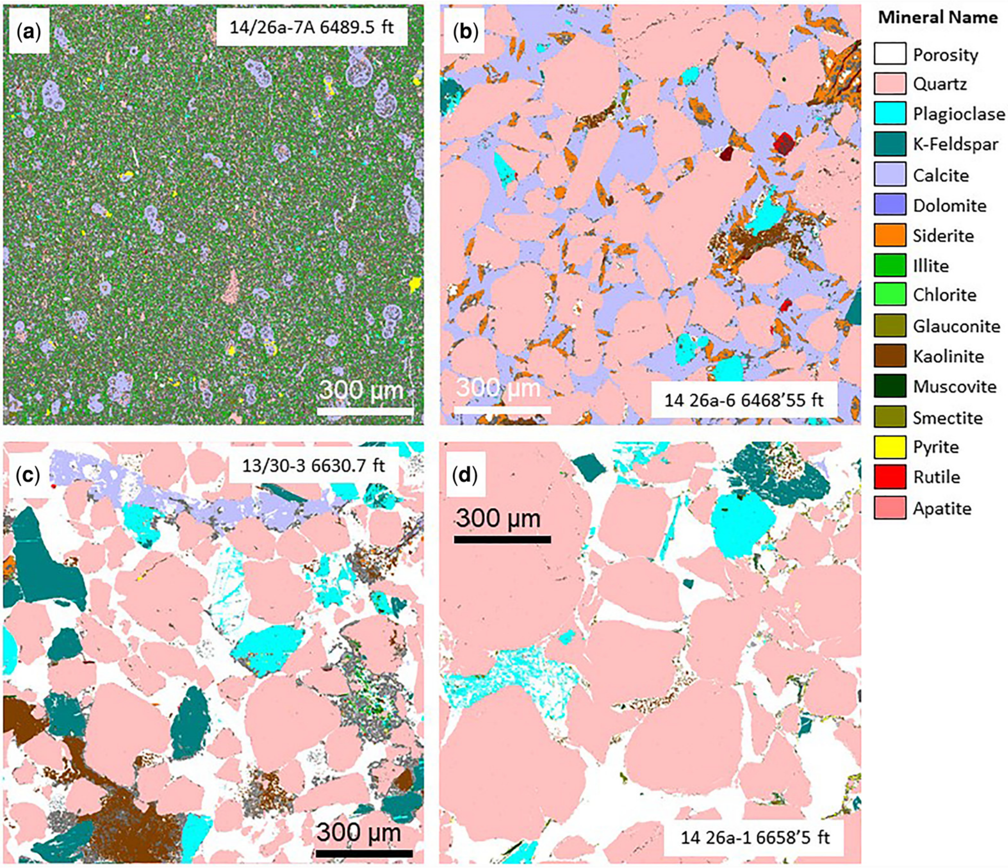

Fig. 12. Typical Scanning electron microscope-energy dispersive spectroscopy (SEM-EDS) images of core samples from Lower Cretaceous storage domain rocks associated with a planned CCS project in the Moray Firth Basin, North Sea, UK. The reservoir section (and see Fig. 4) has variable porosity. The key to the colour scheme is displayed on the right-hand side. (**a**) Rodby Shale dominated by smectite (clay), calcite micro-fossils and minor quartz silt and diagenetic pyrite (Worden *et al.* 2020*a*). SEM-EDS has a minimum resolution of about 1 µm; this sample contains no meso-pores (as expected) and is an excellent potential top-seal to a CO_2-filled reservoir. (**b**) Calcite-cemented sandstone with negligible remaining porosity. The sandstone also contains early diagenetic siderite ($FeCO_3$). This sandstone has very low porosity due to the carbonate cements; this type of rock contributes nothing to the storage potential for the reservoir. (**c**) Medium porosity, poorly sorted sandstone dominated by quartz but with abundant K-feldspar and plagioclase, with localized patches of diagenetic kaolinite and calcite cement derived from a detrital bioclast. (**d**) High porosity sandstone dominated by quartz grains but with minor K-feldspar and plagioclase grains that have undergone dissolution and now contain secondary porosity.

Effect of halite precipitation on permeability

Halite can precipitate within the reservoir at CCS projects where the formation water (brine) has a high saline load (e.g. 20 wt % salinity or more). Brine salinity patterns at the basin and field scale are reasonably well understood, with Na being the dominant cation and Cl being the dominant anion (Worden 1996, 2018). The precipitation of halite, especially in the near-wellbore region, leads to significantly reduced injectivity, thus damaging the efficiency of a CCS reservoir (Bacci *et al.* 2011; Vanorio *et al.* 2011; Miri and Hellevang 2016). The problem of halite formation damage derives from the initial formation water salinity; the specific effect of halite on the pore-network is best studied via experimental simulation of CO_2-induced evaporation of the brine using core samples from the specific reservoir (Muller *et al.* 2009; Sokama-Neuyam *et al.* 2020).

Top-seal properties and core

It is possible to calculate the maximum CO_2 column height by having measurements of capillary entry

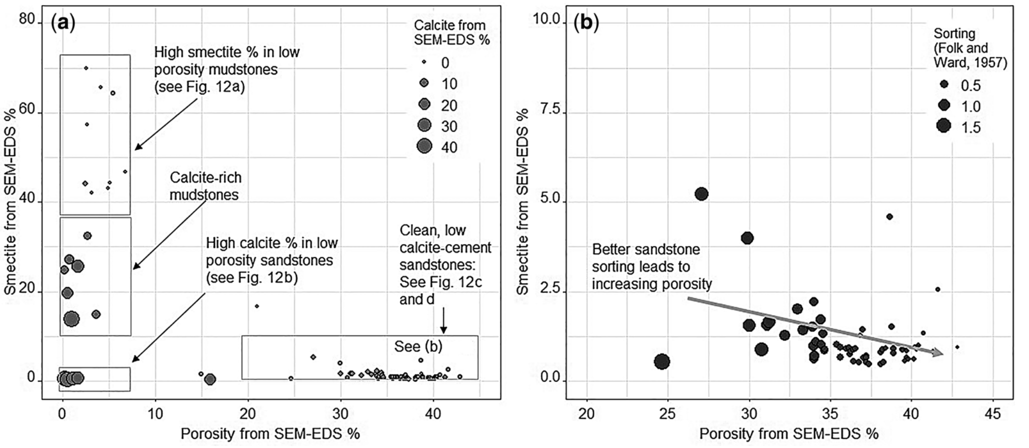

Fig. 13. Quantitative SEM-EDS data from core samples from Lower Cretaceous storage domain rocks associated with a planned CCS project in the Moray Firth Basin, North Sea, UK. (**a**) Porosity v. smectite with symbol size revealing calcite concentration. Porosity (from SEM-EDS image analysis) varies from almost zero to >40% (note that SEM-EDS cannot measure micro-porosity; the low porosity, high smectite mudstones have up to about 14% micro-porosity, as measured using mercury injection porosimetry). Mudstones are rich in smectite compared to other clay minerals. Some of the fine-grained rocks in this formation have relatively high calcite concentrations due to the abundance of calcite microfossils. Rocks with the lowest porosity have negligible smectite as they are clean sandstones that are cemented tight by diagenetic calcite. Rocks with low smectite can have highly variable porosity. (**b**) Enlargement of part of (a), with porosity v. smectite and symbol size revealing the grain size sorting. The highest porosity, clean sandstones have the best sorting (lowest Folk and Ward sorting coefficient), and the lowest porosity sandstones have the worst sorting. Overall, sandstone porosity is influenced by grain sorting and calcite concentrations.

pressure from the top-seal (Armitage *et al.* 2013*b*; Worden *et al.* 2020*a*). Such measurements typically derive from mercury injection porosimetry applied to small rock chips. In theory, mercury injection porosimetry can be undertaken on cuttings samples, but core is preferable as it is possible to relate the data to the exact rock types in its depositional context, and cuttings might not be representative. Mudstones can be highly heterogeneous so that it is useful to use core to relate variable mercury injection porosimetry data to the exact bed type (e.g. proportion of silt, bed thickness or degree of bioturbation).

Diffusive loss of CO_2 through a top-seal depends on porosity and top-seal thickness (Espinoza and Santamarina 2017). Highly credible porosity values and top-seal thicknesses can be acquired from wireline logs so that core is not strictly needed to assess the rate of diffusive CO_2 loss.

Advective loss of CO_2 through a top-seal depends on permeability (and relative permeability), CO_2 viscosity and density, the pressure difference driving flux and top-seal thickness (Espinoza and Santamarina 2017). Permeability in relatively tight top-seal lithologies is typically measured indirectly via mercury injection porosimetry (Armitage *et al.* 2010, 2013*b*). Permeability values from top-seal cannot easily be acquired from logs so that core is useful to measure this key variable, although cuttings can be used for mercury injection porosimetry if not ground to fine rock flour.

As with the CCS reservoir, top-seals may have a rock-specific mineral response to CO_2 injection. For example, calcite-bearing mudstones may undergo dissolution of calcite with a resulting increase in porosity and permeability, and a decrease in rock strength. Similarly, chlorite-bearing mudstones may undergo dissolution, or at least alteration, of chlorite, also with a resulting increase in porosity and permeability and a decrease in rock strength. Conversely, quartz- and illite-bearing mudstones are unlikely to have any sort of response to high CO_2 pressures. Core from top-seal rocks at CCS sites is essential to study mineralogy and rock fabrics (Figs 5 & 12).

Top-seal geomechanical properties, like reservoir geomechanical properties, need to be defined to predict the safe maximum values of fluid pressure to avoid fracture of top-seals. Core is required to make measurements of rock strength.

This new imperative to have good quality core from top-seals, for column height, permeability, rock strength, as well as detailed mineralogy and rock fabric data, represents a significant departure from the priorities of oil and gas exploitation projects that have typically relied on the presence of trapped oil and gas as proof that the top-seal was effective and stable. Note that intraformational baffles as well as top-seals in CCS reservoirs may also need to be studied, ideally using core samples, to address flow properties, reactivity to CO_2, capillary entry pressure, rock strength and geomechanical attributes; this is because intraformational baffles strongly influence the movement patterns of the injected CO_2 and the displacement of pre-existing fluids (Cavanagh and Haszeldine 2014).

Fault rock stability and cores

Fault reactivation has been reported as a risk at high CO_2 pressure (Rutqvist 2012; Zoback and Gorelick 2012). Microseismic activity during CCS projects due to fracturing or fault movement has now been established at several sites such as In Salah in Algeria (Stork *et al.* 2015), Rousse in France (Payre *et al.* 2014) and Decatur, USA (Ringrose *et al.* 2017). Understanding the presence and characteristics of faults, before and during CCS operations, is therefore important. Image and calliper logs have been used to determine stress orientations and, together with downhole measurements such as bleed-off tests and leak-off tests, can be used to determine the stress state of faults with different orientations (Williams *et al.* 2016). Any core collected through CCS reservoir and top-seals needs to be carefully logged for the presence and type of fractures (Wilson *et al.* 2007) to assess the likelihood of the high pressure CO_2 causing movement and opening. Borehole imaging logs can also be used to assess the presence and type of fractures (Williams *et al.* 2016), although image logs can overestimate the number of natural fractures (Fernandez-Ibanez *et al.* 2018).

Conclusions

Many CCS projects will be based in oil- and gas-producing basins, as these have useful infrastructure in place and they have a wealth of knowledge about the subsurface to allow subsurface characterization and ranking of CCS sites (Alcalde *et al.* 2019). Useful first steps are identifying the locations of wells, gathering subsurface data and then establishing which wells have core (Alcalde *et al.* 2021). Many countries have national core repositories and wireline, seismic and drilling data repositories; some companies also store core so that, between these two resources, it should be possible to initiate core-based CCS projects as well as harvest existing data.

Table 1 summarizes the core-based needs, the value of data from archived core and the need for new cores drilled specifically for CCS projects. The usual core data required for oil and gas projects, including reservoir porosity, permeability and sedimentary architecture, can be re-used to assist in CCS projects. Existing core can potentially also be used for the collection of new data specific to CCS projects, including CO_2–brine relative permeability, rock strength and reservoir reactivity to CO_2. Many

Table 1. *Summary of types of data that can be derived from core, the value of archived core and the benefit of collecting new cores when CCS sites have injection (and possibly monitoring) wells drilled*

Core-derived data	Archived core	New core from CCS wells
Typical high-resolution sedimentary core description	Possible based on existing data and core	New data help develop subsurface model
Permeability for modelling injection rate	Possible based on existing data and core	New data help develop subsurface model
Relative permeability of CO_2–brine	Unlikely to be available but possible based on existing core	New data help develop flow models
Geomechanics for safe injection rates	May not be available but possible based on existing core	New data help develop safe injection plan
Local porosity-architecture for modelling near-well bore flow	Possible based on existing data and core	New data help develop subsurface model
Regional porosity model for storage volume	Possible based on existing data	New data help develop subsurface model
Reservoir rock mineral response to high CO_2 pressure	Unlikely to be available but possible based on existing core	New data help develop safe injection plan
Top-seal quality to model CO_2 leakage	Little available	New data needed to confirm seal quality
Top-seal rock mineral response to high CO_2 pressure	Little available	New data needed to confirm seal quality
Reservoir response to drying/salting-out	Little available	New data help develop safe injection plan

oil and gas projects have not focused on top-seals, and it is usual that there is a lack of core from these lithologies. It is likely that there will be a new imperative to collect cores from top-seals at CCS sites; these new cores will be used to define whether the top-seal will leak, react with or be fractured by high pressure CO_2 in the underlying reservoir. New cores collected from CCS reservoirs will also be essential to develop the understanding of the reservoir for flow, storage volume and storage security purposes.

Acknowledgements Reviewer Simon Shoulders and an anonymous reviewer are thanked for helpful and thought-provoking comments on the first version of the paper that led to a better and simpler product. Editor Lucy Williams is thanked for her careful reading of the text and for her insightful suggestions about the tone and emphasis of the paper.

Competing interests The author declares that they have no known competing financial interests or personal relationships that could have appeared to influence the work reported in this paper.

Author contributions **RHW**: conceptualization (lead), data curation (lead), funding acquisition (lead), investigation (lead), visualization (lead), writing – original draft (lead), writing – review & editing (lead).

Funding This research was funded by ERA-NET (Grant No. 271500).

Data availability All data generated or analysed during this study are included in this published article.

References

Alam, M.M., Fabricius, I.L. and Prasad, M. 2011. Permeability prediction in chalks. *American Association of Petroleum Geologists Bulletin*, **95**, 1991–2014, https://doi.org/10.1306/03011110172

Alcalde, J., Heinemann, N. *et al.* 2019. Developing full-chain industrial carbon capture and storage in a resource- and infrastructure-rich hydrocarbon province. *Journal of Cleaner Production*, **233**, 963–971, https://doi.org/10.1016/j.jclepro.2019.06.087

Alcalde, J., Heinemann, N. *et al.* 2021. A criteria-driven approach to the CO_2 storage site selection of East Mey for the Acorn project in the North Sea. *Marine and Petroleum Geology*, **133**, article 105309, https://doi.org/10.1016/j.marpetgeo.2021.105309

Allen, M.J., Faulkner, D.R., Worden, R.H., Rice-Birchall, E., Katirtsidis, N. and Utley, J.E.P. 2020. Geomechanical and petrographic assessment of a CO_2 storage site: application to the Acorn CO_2 storage site, offshore United Kingdom. *International Journal of Greenhouse Gas Control*, **94**, article 102923, https://doi.org/10.1016/j.ijggc.2019.102923

Armitage, P.J., Worden, R.H., Faulkner, D.R., Aplin, A.C., Butcher, A.R. and Iliffe, J. 2010. Diagenetic and sedimentary controls on porosity in Lower Carboniferous fine-grained lithologies, Krechba field, Algeria: a petrological study of a caprock to a carbon capture site. *Marine and Petroleum Geology*, **27**, 1395–1410, https://doi.org/10.1016/j.marpetgeo.2010.03.018

Armitage, P.J., Faulkner, D.R. and Worden, R.H. 2013*a*. Caprock corrosion. *Nature Geoscience*, **6**, 79–80, https://doi.org/10.1038/ngeo1716

Armitage, P.J., Worden, R.H., Faulkner, D.R., Aplin, A.C., Butcher, A.R. and Espie, A.A. 2013*b*. Mercia Mudstone Formation caprock to carbon capture and storage sites: petrology and petrophysical characteristics. *Journal of the Geological Society, London*, **170**, 119–132, https://doi.org/10.1144/jgs2012-049

Bacci, G., Korre, A. and Durucan, S. 2011. An experimental and numerical investigation into the impact of dissolution/precipitation mechanisms on CO_2 injectivity in the wellbore and far field regions. *International Journal of Greenhouse Gas Control*, **5**, 579–588, https://doi.org/10.1016/j.ijggc.2010.05.007

Betts, R. 2021. Met Office: atmospheric CO_2 now hitting 50% higher than pre-industrial levels, https://www.carbonbrief.org/met-office-atmospheric-co2-now-hitting-50-higher-than-pre-industrial-levels [last accessed 31 January 2022].

Blake, O.O., Faulkner, D.R., Worden, R.H., Armitage, P.J. and Espie, A.A. 2022. Reservoir and caprock fracturing due to thermal shock unlikely to result from CO_2 injection during CCS: experimental evidence. *International Journal of Greenhouse Gas Control*, **118**, article 103691, https://doi.org/10.1016/j.ijggc.2022.103691

Burnside, N.M. and Naylor, M. 2014. Review and implications of relative permeability of CO_2/brine systems and residual trapping of CO_2. *International Journal of Greenhouse Gas Control*, **23**, 1–11, https://doi.org/10.1016/j.ijggc.2014.01.013

Busch, A., Hangx, S.J.T., Marshall, J.D. and Wentinck, H.M. 2020. Swelling clay minerals and containment risk assessment for the storage seal of the Peterhead CCS project. *International Journal of Greenhouse Gas Control*, **94**, article 102924, https://doi.org/10.1016/j.ijggc.2019.102924

Cade, C.A., Evans, I.J. and Bryant, S.L. 1994. Analysis of permeability controls – a new approach. *Clay Minerals*, **29**, 491–501, https://doi.org/10.1180/claymin.1994.029.4.08

Cannon, S. 2016. *Petrophysics – a Practical Guide*. Wiley, Chichester.

Carey, J.W., Wigand, M. *et al.* 2007. Analysis and performance of oil well cement with 30 years of CO_2 exposure from the SACROC Unit, West Texas, USA. *International Journal of Greenhouse Gas Control*, **1**, 75–85, https://doi.org/10.1016/s1750-5836(06)00004-1

Cavanagh, A.J. and Haszeldine, R.S. 2014. The Sleipner storage site: capillary flow modeling of a layered CO_2 plume requires fractured shale barriers within the Utsira Formation. *International Journal of Greenhouse Gas Control*, **21**, 101–112, https://doi.org/10.1016/j.ijggc.2013.11.017

Chang, C.D., Zoback, M.D. and Khaksar, A. 2006. Empirical relations between rock strength and physical properties in sedimentary rocks. *Journal of Petroleum Science and Engineering*, **51**, 223–237, https://doi.org/10.1016/j.petrol.2006.01.003

Clark, D.E., Oelkers, E.H., Gunnarsson, I., Sigfusson, B., Snaebjornsdottir, S.O., Aradottir, E.S. and Gislason, S.R. 2020. CarbFix2: CO_2 and H_2S mineralization during 3.5 years of continuous injection into basaltic rocks at more than 250°C. *Geochimica et Cosmochimica Acta*, **279**, 45–66, https://doi.org/10.1016/j.gca.2020.03.039

Dawson, G.K.W., Pearce, J.K., Biddle, D. and Golding, S.D. 2015. Experimental mineral dissolution in Berea Sandstone reacted with CO_2 or SO_2-CO_2 in NaCl brine under CO_2 sequestration conditions. *Chemical Geology*, **399**, 87–97, https://doi.org/10.1016/j.chemgeo.2014.10.005

Dean, M. and Tucker, O.D. 2017. A risk-based framework for measurement, monitoring and verification (MMV) of the Goldeneye storage complex for the Peterhead CCS project, UK. *International Journal of Greenhouse Gas Control*, **61**, 1–15, https://doi.org/10.1016/j.ijggc.2017.03.014

Doughty, C., Freifeld, B.M. and Trautz, R.C. 2008. Site characterization for CO_2 geologic storage and vice versa: the Frio brine pilot, Texas, USA as a case study. *Environmental Geology*, **54**, 1635–1656, https://doi.org/10.1007/s00254-007-0942-0

Espinoza, D.N. and Santamarina, J.C. 2017. CO_2 breakthrough-caprock sealing efficiency and integrity for carbon geological storage. *International Journal of Greenhouse Gas Control*, **66**, 218–229, https://doi.org/10.1016/j.ijggc.2017.09.019

Fernandez-Ibanez, F., Degraff, J. and Ibrayev, F. 2018. Integrating borehole image logs with core: a method to enhance subsurface fracture characterization. *American Association of Petroleum Geologists Bulletin*, **102**, 1067–1090, https://doi.org/10.1306/0726171609317002

Folk, R.L. and Ward, W.C. 1957. Brazos river bar. A study in the significance of grain size parameters. *Journal of Sedimentary Petrology*, **27**, 3–26, https://doi.org/10.1306/74D70646-2B21-11D7-8648000102C1865D

Gaarenstroom, L., Tromp, R.A.J., de Jong, M.C. and Brandenburg, A.M. 1993. Overpressures in the central North Sea: implications for trap integrity and drilling safety. *Geological Society, London, Petroleum Geology Conference Series*, **4**, 1305–1313, https://doi.org/10.1144/0041305

Gholami, R., Raza, A. and Iglauer, S. 2021. Leakage risk assessment of a CO_2 storage site: a review. *Earth-Science Reviews*, **223**, article 103849, https://doi.org/10.1016/j.earscirev.2021.103849

Global CCS Institute 2022. *Global Status of CCS 2021*. Global CCS Institute.

Goertz-Allmann, B.P., Kuhn, D., Oye, V., Bohloli, B. and Aker, E. 2014. Combining microseismic and geomechanical observations to interpret storage integrity at the In Salah CCS site. *Geophysical Journal International*, **198**, 447–461, https://doi.org/10.1093/gji/ggu010

Graven, H., Allison, C.E. *et al*. 2017. Compiled records of carbon isotopes in atmospheric CO_2 for historical simulations in CMIP6. *Geoscientific Model Development*, **10**, 4405–4417, https://doi.org/10.5194/gmd-10-4405-2017

Grude, S., Landro, M. and Dvorkin, J. 2014. Pressure effects caused by CO_2 injection in the Tubåen Fm., the Snøhvit field. *International Journal of Greenhouse Gas Control*, **27**, 178–187, https://doi.org/10.1016/j.ijggc.2014.05.013

Hangx, S., van der Linden, A., Marcelis, F. and Bauer, A. 2013. The effect of CO_2 on the mechanical properties of the Captain Sandstone: geological storage of CO_2 at the Goldeneye Field (UK). *International Journal of Greenhouse Gas Control*, **19**, 609–619, https://doi.org/10.1016/j.ijggc.2012.12.016

Hansen, O., Gilding, D. *et al*. 2013. Snøhvit: the history of injecting and storing 1 Mt CO_2 in the fluvial Tubåen Fm. *Energy Procedia*, **37**, 3565–3573, https://doi.org/10.1016/j.egypro.2013.06.249

Hughes, D.S. 2008. Carbon storage in depleted gas fields: key challenges. *In*: *9th International Conference on Greenhouse Gas Control Technologies*, 16–20 November, Washington, DC, 3007–3014.

Iglauer, S., Paluszny, A., Rahman, T., Zhang, Y.H., Wulling, W. and Lebedev, M. 2019. Residual trapping of CO_2 in an oil-filled, oil-wet sandstone core: results of three-phase pore-scale imaging. *Geophysical Research Letters*, **46**, 11146–11154, https://doi.org/10.1029/2019gl083401

Jahn, F., Cook, M. and Graham, C. 2008. *Hydrocarbon Exploration and Production*. 2nd edn. Elsevier, Amsterdam.

James, A., Baines, S. and McCollough, S. 2016*a*. *Progressing Development of the UK's Strategic Carbon Dioxide Storage Resource: a Summary of Results from the Strategic UK CO_2 Storage Appraisal Project*. The Energy Technologies Institute, Loughborough.

James, A., Baines, S. and McCollough, S. 2016*b*. *Strategic UK CCS Storage Appraisal – WP5C – Hamilton Storage Development Plan*. Energy Technologies Institute, Loughborough.

Kaldi, J.G., Daniel, R.F. *et al*. 2011. *Caprock Systems for Geological Storage of CO_2*. Cooperative Research Centre for Greenhouse Gas Technologies.

Kaldi, J.G., Daniel, R.F. *et al*. 2013. Containment of CO_2 in CCS: role of caprocks and faults. *Energy Procedia*, **37**, 5403–5410, https://doi.org/10.1016/j.egypro.2013.06.458

Kelly, S., Worden, R.H. and McArdle, P. 2022. The value of core in mature field development – examples from the UK North Sea. *Geological Society, London, Special Publications*, **527**, https://doi.org/10.1144/SP527-2021-203

Krevor, S.C.M., Pini, R., Zuo, L. and Benson, S.M. 2012. Relative permeability and trapping of CO_2 and water in sandstone rocks at reservoir conditions. *Water Resources Research*, **48**, https://doi.org/10.1029/2011wr010859

Lake, L.W., Lotfollahi, M. and Bryant, S. 2019. CO_2 enhanced oil recovery experience and its messages for CO_2 storage. *In*: Newell, P. and Ilgen, G.A. (eds) *Science of Carbon Storage in Deep Saline Aquifers*. Elsevier, Amsterdam, 15–31.

Lau, H.C., Ramakrishna, S., Zhang, K. and Radhamani, A.V. 2021. The role of carbon capture and storage in the energy transition. *Energy & Fuels*, **35**, 7364–7386, https://doi.org/10.1021/acs.energyfuels.1c00032

Lescanne, M., Hy-Billiot, J., Aimard, N. and Prinet, C. 2011. The site monitoring of the Lacq industrial CCS reference project. *Energy Procedia*, **4**, 3518–3525, https://doi.org/10.1016/j.egypro.2011.02.279

Liu, H. 2017. *Principles and Applications of Well Logging*. Springer, Berlin.

Loring, J.S., Miller, Q.R.S., Thompson, C.J. and Schaef, H.T. 2019. Experimental studies of reactivity and transformations of rocks and minerals in water-bearing supercritical CO_2. *In*: Newell, P. and Ilgen, G.A. (eds) *Science of Carbon Storage in Deep Saline Aquifers*. Elsevier, Amsterdam, 63–88.

Mahabadi, N., van Paassen, L., Battiato, I., Yun, T.S., Choo, H. and Jang, J. 2020. Impact of pore-scale characteristics on immiscible fluid displacement. *Geofluids*, **2020**, article 5759023, https://doi.org/10.1155/2020/5759023

Marshall, J.D., Tucker, O.D. and Lovelock, C.E. 2016. Goldeneye: modelling a depleted field for carbon capture – how much uncertainty is left? *Petroleum Geoscience*, **22**, 37–45, https://doi.org/10.1144/petgeo2014-072

Miri, R. and Hellevang, H. 2016. Salt precipitation during CO_2 storage – a review. *International Journal of Greenhouse Gas Control*, **51**, 136–147, https://doi.org/10.1016/j.ijggc.2016.05.015

Miri, R. and Hellevang, H. 2019. Critical Factors for Considering CO_2 Injectivity in Saline Aquifers. *FME SUCCESS Synthesis report*, **3**.

Miri, R., van Noort, R., Aagaard, P. and Hellevang, H. 2015. New insights on the physics of salt precipitation during injection of CO_2 into saline aquifers. *International Journal of Greenhouse Gas Control*, **43**, 10–21, https://doi.org/10.1016/j.ijggc.2015.10.004

Mito, S., Xue, Z.Q. and Ohsumi, T. 2008. Case study of geochemical reactions at the Nagaoka CO_2 injection site, Japan. *International Journal of Greenhouse Gas Control*, **2**, 309–318, https://doi.org/10.1016/j.ijggc.2008.04.007

Mito, S., Xue, Z.Q. and Satoh, H. 2015. Experimental assessment of well integrity for CO_2 geological storage: batch experimental results on geochemical interactions between a CO_2–brine mixture and a sandstone–cement–steel sample. *International Journal of Greenhouse Gas Control*, **39**, 420–431, https://doi.org/10.1016/j.ijggc.2015.06.007

Muller, N., Qi, R., Mackie, E., Pruess, K. and Blunt, M.J. 2009. CO_2 injection impairment due to halite precipitation. *Energy Procedia*, **1**, 3507–3514, https://doi.org/10.1016/j.egypro.2009.02.143

Nordbotten, J.M. and Celia, M.A. 2006. *Geological Storage of CO_2: Modelling Approaches for Large Scale Simulation*. Wiley, Chichester.

Nover, G., von der Gonna, J., Heikamp, S. and Koster, J. 2013. Changes of petrophysical properties of sandstones due to interaction with supercritical carbon dioxide – a laboratory study. *European Journal of Mineralogy*, **25**, 317–329, https://doi.org/10.1127/0935-1221/2013/0025-2295

Okwen, R.T., Stewart, M.T. and Cunningham, J.A. 2010. Analytical solution for estimating storage efficiency of geologic sequestration of CO_2. *International Journal of Greenhouse Gas Control*, **4**, 102–107, https://doi.org/10.1016/j.ijggc.2009.11.002

Oldenburg, C.M. 2007. Joule–Thomson cooling due to CO_2 injection into natural gas reservoirs. *Energy Conversion and Management*, **48**, 1808–1815, https://doi.org/10.1016/j.enconman.2007.01.010

Payre, X., Maisons, C., Marble, A. and Thibeau, S. 2014. Analysis of the passive seismic monitoring performance at the Rousse CO_2 storage demonstration pilot. *Energy Procedia*, **63**, 4339–4357, https://doi.org/10.1016/j.egypro.2014.11.469

Plennevaux, C., Ferrando, N. *et al*. 2013. pH prediction in concentrated aqueous solutions under high pressure of acid gases and high temperature. *Corrosion Science*, **73**, 143–149, https://doi.org/10.1016/j.corsci.2013.04.002

Preston, C., Monea, M. *et al*. 2005. IEA GHG Weyburn CO_2 monitoring and storage project. *Fuel Processing Technology*, **86**, 1547–1568, https://doi.org/10.1016/j.fuproc.2005.01.019

Rider, M. and Kennedy, M.J. 2011. *The Geological Interpretation of Well Logs*. Rider-French Consulting, Cambridge, UK.

Ringrose, P. 2020. *How to Store CO_2 Underground: Insights from Early-Mover CCS Projects*. Springer, Switzerland.

Ringrose, P., Greenberg, S., Whittaker, S., Nazarian, B. and Oye, V. 2017. Building confidence in CO_2 storage using reference datasets from demonstration projects. *Energy Procedia*, **114**, 3547–3557, https://doi.org/10.1016/j.egypro.2017.03.1484

Rohde, R. 2021. Global temperature report for 2020, http://berkeleyearth.org/global-temperature-report-for-2020/ [last accessed 31 January 2022].

Rutqvist, J. 2012. The geomechanics of CO_2 storage in deep sedimentary formations. *Geotechnical and Geological Engineering*, **30**, 525–551, https://doi.org/10.1007/s10706-011-9491-0

Rutqvist, J., Vasco, D.W. and Myer, L. 2010. Coupled reservoir-geomechanical analysis of CO_2 injection and ground deformations at In Salah, Algeria. *International Journal of Greenhouse Gas Control*, **4**, 225–230, https://doi.org/10.1016/j.ijggc.2009.10.017

Rybacki, E., Reinicke, A., Meier, T., Makasi, M. and Dresen, G. 2015. What controls the mechanical properties of shale rocks? – part I: strength and Young's modulus. *Journal of Petroleum Science and Engineering*, **135**, 702–722, https://doi.org/10.1016/j.petrol.2015.10.028

Rybacki, E., Meier, T. and Dresen, G. 2016. What controls the mechanical properties of shale rocks? – part II: brittleness. *Journal of Petroleum Science and Engineering*, **144**, 39–58, https://doi.org/10.1016/j.petrol.2016.02.022

Santarelli, F.J., Tronvoll, J.T., Svennekjaer, M., Skeie, H., Henriksen, R. and Bratli, R.K. 1999. Reservoir stress path: the depletion and the rebound. *In*: *SPE/ISRM Rock Mechanics in Petroleum Engineering Conference*, 8–10 July 1998, Trondheim, Norway, 203–209.

Shevalier, M., Nightingale, M., Mayer, B., Hutcheon, I., Durocher, K. and Perkins, E. 2013. Brine geochemistry changes induced by CO_2 injection observed over a 10 year period in the Weyburn oil field. *International Journal of Greenhouse Gas Control*, **16**, S160–S176, https://doi.org/10.1016/j.ijggc.2013.02.017

Shin, H. and Santamarina, J.C. 2017. Sediment–well interaction during depressurization. *Acta Geotechnica*, **12**, 883–895, https://doi.org/10.1007/s11440-016-0493-1

Singh, K., Anabaraonye, B.U., Blunt, M.J. and Crawshaw, J. 2018. Partial dissolution of carbonate rock grains during reactive CO_2-saturated brine injection under reservoir conditions. *Advances in Water Resources*, **122**, 27–36, https://doi.org/10.1016/j.advwatres.2018.09.005

Snaebjornsdottir, S.O., Oelkers, E.H. *et al*. 2017. The chemistry and saturation states of subsurface fluids during the in situ mineralisation of CO_2 and H_2S at the CarbFix site in SW-Iceland. *International Journal of Greenhouse Gas Control*, **58**, 87–102, https://doi.org/10.1016/j.ijggc.2017.01.007

Snaebjornsdottir, S.O., Gislason, S.R., Galeczka, I.M. and Oelkers, E.H. 2018. Reaction path modelling of in-situ mineralisation of CO_2 at the CarbFix site at Hellisheidi, SW-Iceland. *Geochimica et Cosmochimica Acta*, **220**, 348–366, https://doi.org/10.1016/j.gca.2017.09.053

Sokama-Neuyam, Y.A., Ursin, J.R. and Boakye, P. 2020. Experimental investigation of the mechanism of salt precipitation during CO_2 injection in sandstone. *Journal of Carbon Research*, **5**, 4, https://doi.org/10.3390/c5010004

Stork, A.L., Verdon, J.P. and Kendall, J.M. 2015. The microseismic response at the In Salah carbon capture and storage (CCS) site. *International Journal of Greenhouse Gas Control*, **32**, 159–171, https://doi.org/10.1016/j.ijggc.2014.11.014

Sundal, A. and Hellevang, H. 2019. Using reservoir geology and petrographic observations to improve CO_2 mineralization estimates: examples from the Johansen Formation, North Sea, Norway. *Minerals*, **9**, 671, https://doi.org/10.3390/min9110671

Szabo, Z., Hellevang, H. *et al*. 2016. Experimental-modelling geochemical study of potential CCS caprocks in brine and CO_2-saturated brine. *International Journal of Greenhouse Gas Control*, **44**, 262–275, https://doi.org/10.1016/j.ijggc.2015.11.027

United Nations Intergovernmental Panel on Climate Change 2005. *Special Report on Carbon Dioxide Capture and Storage*. Cambridge University Press.

Vanorio, T., Nur, A. and Ebert, Y. 2011. Rock physics analysis and time-lapse rock imaging of geochemical effects due to the injection of CO_2 into reservoir rocks. *Geophysics*, **76**, O23–O33, https://doi.org/10.1190/geo2010-0390.1

Verdon,, J.P. 2016. Using microseismic data recorded at the Weyburn CCS-EOR site to assess the likelihood of induced seismic activity. *International Journal of Greenhouse Gas Control*, **54**, 421–428, https://doi.org/10.1016/j.ijggc.2016.03.018

Verdon, J.P., Kendall, J.M. and Maxwell, S.C. 2010. A comparison of passive seismic monitoring of fracture stimulation from water and CO_2 injection. *Geophysics*, **75**, MA1–MA7, https://doi.org/10.1190/1.3377789

Verdon, J.P., Kendall, J.M., White, D.J. and Angus, D.A. 2011. Linking microseismic event observations with geomechanical models to minimise the risks of storing CO_2 in geological formations. *Earth and Planetary Science Letters*, **305**, 143–152, https://doi.org/10.1016/j.epsl.2011.02.048

Vilarrasa, V., Makhnenko, R.Y. and Rutqvist, J. 2019. Field and laboratory studies of geomechanical response to the injection of CO_2. *In*: Newell, P. and Ilgen, G.A. (eds) *Science of Carbon Storage in Deep Saline Aquifers*. Elsevier, Amsterdam, 209–236.

Wei, B., Zhang, X., Liu, J., Xu, X.G., Pu, W.F. and Bai, M.X. 2020. Adsorptive behaviors of supercritical CO_2 in tight porous media and triggered chemical reactions with rock minerals during CO_2-EOR and -sequestration. *Chemical Engineering Journal*, **381**, article 122577, https://doi.org/10.1016/j.cej.2019.122577

Williams, G.A. and Chadwick, R.A. 2021. Influence of reservoir-scale heterogeneities on the growth, evolution and migration of a CO_2 plume at the Sleipner Field, Norwegian North Sea. *International Journal of Greenhouse Gas Control*, **106**, article 103260, https://doi.org/10.1016/j.ijggc.2021.103260

Williams, J.D.O., Fellgett, M.W. and Quinn, M.F. 2016. Carbon dioxide storage in the Captain Sandstone aquifer: determination of in situ stresses and fault-stability analysis. *Petroleum Geoscience*, **22**, 211–222, https://doi.org/10.1144/petgeo2016-036

Wilson, T., Paulsen, T., Laufer, A.L. and Millan, C. 2007. Fracture logging of the AND-1B core, McMurdo Ice Shelf project, Antarctica. *Terra Antarctica*, **14**, 175–184.

Wolf, J.L., Niemi, A., Bensabat, J. and Rebscher, D. 2016. Benefits and restrictions of 2D reactive transport simulations of CO_2 and SO_2 co-injection into a saline aquifer using TOUGHREACT V3.0-OMP. *International Journal of Greenhouse Gas Control*, **54**, 610–626, https://doi.org/10.1016/j.ijggc.2016.07.005

Worden, R.H. 1996. Controls on halogen concentrations in sedimentary formation waters. *Mineralogical Magazine*, **60**, 259–274, https://doi.org/10.1180/minmag.1996.060.399.02

Worden, R.H. 2018. Halogen elements in sedimentary systems and their evolution during diagenesis. *In*: Harlov, D.E. and Aranovich, L. (eds) *Role of Halogens in Terrestrial and Extraterrestrial Processes: Surface Crust and Mantle*. Springer, Berlin, 185–260.

Worden, R.H. and Smith, L.K. 2004. Geological sequestration of CO_2 in the subsurface: lessons from CO_2 injection enhanced oil recovery projects in oilfields. *Geological Society, London, Special Publications*, **233**, 211–224, https://doi.org/10.1144/gsl.sp.2004.233.01.14

Worden, R.H., Armitage, P.J. *et al*. 2018. Petroleum reservoir quality prediction: overview and contrasting approaches from sandstone and carbonate communities. *Geological Society, London, Special Publications*, **435**, 1–31, https://doi.org/10.1144/SP435.21

Worden, R.H., Allen, M.J. *et al*. 2020*a*. Lower Cretaceous Rodby and Palaeocene Lista shales: characterisation and comparison of top-seal mudstones at two planned CCS sites, offshore UK. *Minerals*, **10**, 691, https://doi.org/10.3390/min10080691

Worden, R.H., Griffiths, J. *et al*. 2020*b*. Chlorite in sandstones. *Earth-Science Reviews*, **204**, article 103105, https://doi.org/10.1016/j.earscirev.2020.103105

Worth, K., White, D. *et al*. 2014. Aquistore project measurement, monitoring, and verification: from concept to CO_2 injection. *Energy Procedia*, **63**, 3202–3208, https://doi.org/10.1016/j.egypro.2014.11.345

Xu, T.F., Apps, J.A., Pruess, K. and Yamamoto, H. 2007. Numerical modeling of injection and mineral trapping of CO_2 with H_2S and SO_2 in a sandstone formation.

Chemical Geology, **242**, 319–346, https://doi.org/10.1016/j.chemgeo.2007.03.022

Yang, G.D., Li, Y.L., Atrens, A., Yu, Y. and Wang, Y.S. 2017. Numerical investigation into the impact of CO_2–water–rock interactions on CO_2 injectivity at the Shenhua CCS Demonstration project, China. *Geofluids*, **2017**, article 4278621, https://doi.org/10.1155/2017/4278621

Zhang, R. and Wu, Y.-S. 2019. Hydrologic, mechanical, thermal, and chemical process coupling triggered by the injection of CO_2. *In*: Newell, P. and Ilgen, G.A. (eds) *Science of Carbon Storage in Deep Saline Aquifers*. Elsevier, Amsterdam, 361–381.

Zhou, Q.L., Birkholzer, J.T., Tsang, C.F. and Rutqvist, J. 2008. A method for quick assessment of CO_2 storage capacity in closed and semi-closed saline formations. *International Journal of Greenhouse Gas Control*, **2**, 626–639, https://doi.org/10.1016/j.ijggc.2008.02.004

Zoback, M.D. 2007. *Reservoir Geomechanics*. Cambridge University Press, Cambridge.

Zoback, M.D. and Gorelick, S.M. 2012. Earthquake triggering and large-scale geologic storage of carbon dioxide. *Proceedings of the National Academy of Sciences of the United States of America*, **109**, 10164–10168, https://doi.org/10.1073/pnas.1202473109